

Structures of nanometre-size crystals determined  
from selected-area electron diffraction dataThomas E. Weirich,<sup>a,\*†2</sup> Xiaodong Zou,<sup>a</sup> Reiner Ramlau,<sup>b</sup> Arndt Simon,<sup>b</sup>  
Giovanni Luca Cascarano,<sup>c</sup> Carmelo Giacovazzo<sup>c</sup> and Sven Hovmöller<sup>a</sup><sup>a</sup>Structural Chemistry, Stockholm University, S-106 91 Stockholm, Sweden, <sup>b</sup>Max-Planck-Institut für Festkörperforschung, Heisenbergstrasse 1, D-70569 Stuttgart, Germany, and <sup>c</sup>Istituto di Ricerca per lo Sviluppo di Metodologie Cristallografiche, CNR c/o Dipartimento Geomineralogico, Campus Universitario, Via E. Orabona 4, 70125 Bari, Italy. Correspondence e-mail: weirich@hrzpub.tu-darmstadt.de

The structure of a new modification of Ti<sub>2</sub>Se, the  $\beta$ -phase, and several related inorganic crystal structures containing elements with atomic numbers between 16 and 40 have been solved by quasi-automatic direct methods from single-crystal electron diffraction patterns of nanometre-size crystals, using the kinematical approximation. The crystals were several thousand times smaller than the minimum size required for single-crystal X-ray diffraction. Atomic coordinates were found with an average accuracy of 0.2 Å or better. Experimental data were obtained by standardized techniques for recording and quantifying electron diffraction patterns. The *SIR97* program for solving crystal structures from three-dimensional X-ray diffraction data by direct methods was modified to work also with two-dimensional electron diffraction data.

© 2000 International Union of Crystallography  
Printed in Great Britain – all rights reserved

## 1. Introduction

The atomic structure is a key factor for understanding the macroscopic properties of materials. This is essential for improving existing and tailoring new materials with special characteristics. In particular, the unusual properties of nanometre-sized crystals have become a topic of great importance in materials science. The need to determine structures of such tiny crystals, however, faces the problem that single-crystal X-ray diffraction cannot be applied owing to the small crystal size. Even the intense beam of a modern synchrotron is not sufficient for crystals smaller than several cubic micrometres. Electrons interact many thousand times more strongly with matter than X-rays do and so are the only alternative for studying the structure of such small crystals.

High-resolution electron microscopy (HREM) is a very useful method for solving unknown crystal structures (Weirich, Ramlau *et al.*, 1996), especially since the crystallographic structure-factor phases which are lost in diffraction patterns are preserved in the electron-microscopy images and can be extracted easily from the Fourier transforms (DeRosier & Klug, 1968). However, HREM is a very demanding technique and it is not always possible to obtain good images with better than 2 Å resolution, especially from beam-sensitive

materials. In contrast, selected-area electron diffraction (SAED) patterns can usually be obtained with sufficient quality better than 1 Å resolution from most compounds in a standard transmission electron microscope. This also includes beam-sensitive materials. For these reasons, it would be highly desirable if unknown crystal structures could be solved directly from electron diffraction patterns.

Direct methods have been successfully applied for solving organic crystal structures from electron diffraction data (Dorset, 1995, 1996, 1998). However, only very few attempts have been made on inorganic compounds, and these have been on data sets collected as texture patterns, a technique which unfortunately is only mastered in very few laboratories, notably those related to the pioneers of electron crystallography in Moscow (Vainshtein *et al.*, 1992). Recently, the structures of several unknown compounds including zeolites (Nicolopoulos *et al.*, 1995), ceramic oxides (Sinkler *et al.*, 1998) and a precipitate Al<sub>m</sub>Fe in aluminium alloys (Gjønnnes *et al.*, 1998) have been solved by exploiting electron diffraction data.

Metal-rich compounds of the early transition metals with *p* elements form a variety of complex structures with extended regions of metal–metal (*M–M*) contacts. These regions frequently contain octahedral *M*<sub>6</sub> clusters which are linked (condensed) *via* common corners, edges and/or faces. Structures containing condensed metal clusters often exhibit interesting physical properties including superconductivity (Simon, 1997). In a recent study on systems with the metals Ti, Zr or Ta and non-metals S, Se and P, many compounds had

† Present address: Technische Universität Darmstadt, Fachbereich Materialwissenschaft, Fachgebiet Strukturforchung, Petersenstrasse 23, D-64287 Darmstadt, Germany.

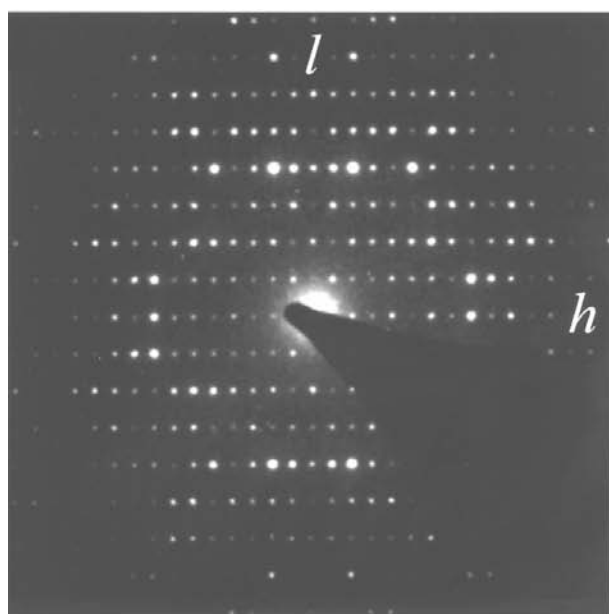
been synthesized and their structures solved, either by X-ray single-crystal diffraction and/or by HREM combined with crystallographic image processing (Weirich, 1996). We show here that a hitherto unknown crystal structure in the Ti–Se system,  $\beta$ -Ti<sub>2</sub>Se, and structures of several other related metal-rich compounds can be solved from SAED data collected with standard instruments using a standard program for direct methods, *SIR97*.

## 2. Sample

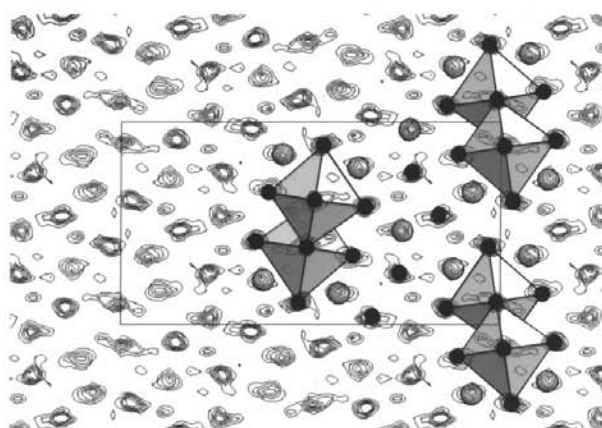
High-temperature treatment of a sample with nominal composition Ti:Se = 8:3 resulted in a microcrystalline powder. From the X-ray powder diffraction, it was clear that the sample contained several phases. The diffuse lines in the powder diffractogram indicated small grain sizes and correspondingly no crystals large enough for single-crystal X-ray diffraction could be found. All attempts to index the

X-ray powder diffraction pattern or to identify the unknown phases from it failed. However, examination of the sample by transmission electron microscopy and energy-dispersive X-ray spectroscopy (EDXS, Tracor Voyager) showed the presence of two hitherto unknown compounds. For one of the compounds, Ti<sub>45</sub>Se<sub>16</sub>, it was possible to find thin crystallites so that the structure could be solved from HREM images after applying crystallographic image processing (Weirich, 1996). In the case of the new modification  $\beta$ -Ti<sub>2</sub>Se, it was not possible to find crystals thin enough to obtain good HREM images. Consequentially, we attempted to solve the structure by direct methods from selected-area electron diffraction data.

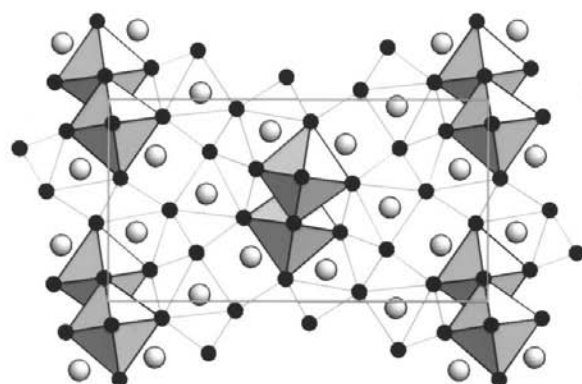
The sample was crushed and studied in a Philips CM30/ST transmission electron microscope operated at 300 kV. SAED patterns were recorded from a crystal with dimensions about 80 × 90 nm in projection, by a slow-scan CCD camera (1024<sup>2</sup> pixel area, model Gatan 694) and on standard photographic EM films (Fig. 1*a*).



(a)



(b)



(c)

**Figure 1**

(*a*) A SAED pattern of  $\beta$ -Ti<sub>2</sub>Se taken along the short *b* axis. The reflections with even indices along the *h* and *l* axes are clearly stronger than those with odd indices. This points to the projected symmetry *p2gg*, for which the odd axial reflections are extinct. The presence of weak intensities in some forbidden reflections is due to multiple (dynamical) scattering. (*b*) Potential map for  $\beta$ -Ti<sub>2</sub>Se obtained by direct methods using the quantified *h0l* electron diffraction data in (*a*). The map shows the potential distribution projected along the *b* axis. The peaks in the map were assigned to Ti atoms (filled circles) and Se atoms (open circles). The condensed Ti<sub>6</sub> clusters are indicated as edge-sharing octahedra. (*c*) Structure model of  $\beta$ -Ti<sub>2</sub>Se after least-squares structure refinement. Most of the Ti atoms are in metal clusters while all Se atoms are isolated inside trigonal prisms.

### 3. Methods and results

$\beta$ -Ti<sub>2</sub>Se has a primitive orthorhombic unit cell with approximate lattice parameters  $a = 17.9$ ,  $b = 3.5$  and  $c = 9.5$  Å. SAED patterns from two different zone axes of known relative crystal tilt angle (goniometer tilt about 43°) were used for determining the crystal system, the lattice type and the lattice parameters. The SAED patterns mentioned above were recorded from [010] and [16 $\bar{1}$ ] zone axes. The approximate  $a$  and  $c$  lattice parameters were improved by averaging three calibrated SAED patterns taken along the [010] zone axis. A more accurate  $b$  parameter was obtained from the solitary (020) peak, which could be identified from X-ray powder diffraction.

The ( $h0l$ ) diffraction patterns showed extinctions ( $h00$ ):  $h = 2n+1$  and ( $00l$ ):  $l = 2n+1$ , compatible with the space groups  $Pc2a$  (No. 32),  $Pn2_1a$  (No. 33),  $Pn2n$  (No. 34),  $Pcma$  (No. 55),  $Pnmm$  (No. 58) and  $Pnma$  (No. 62). Each of the possible space groups was tried in *SIR97* and a trial structure was proposed by direct methods. A subsequent analysis of these structures indicated that the correct space group was  $Pnma$ , since it gave the most chemically reasonable three-dimensional structure.

Electron diffraction intensities were extracted from a SAED pattern of  $\beta$ -Ti<sub>2</sub>Se taken along the short  $b$  axis using the ELD system (Zou *et al.*, 1993). Symmetry-related reflections were merged and the data then fed into the program *SIR97* (Giacovazzo, 1998; Altomare *et al.*, 1999), with atomic scattering factors for electrons (Jiang & Li, 1984).

Dynamical diffraction was taken into account using the approximation  $|F_{hkl}| \propto I_{hkl}$  (Vainshtein, 1964; Cowley, 1992), where  $I_{hkl}$  are intensities extracted by ELD. Although previously only applied for correcting electron diffraction data from mosaic crystals and polycrystalline specimens, we note that this type of correction improved also the quality of the single-crystal data obtained in this investigation.

*SIR97* uses the multiresolution procedure, starting from several different starting phase sets and ending up with equally many solutions. A number of figures of merit were calculated and integrated into the combined figures of merit (CFOM). The solution with the highest CFOM gave a potential map with all atoms and the correct projected structure (Fig. 1*b*). This map showed 36 strong peaks in the unit cell, 24 of which could be assigned to Ti and the other 12 to Se (6 Ti and 3 Se atoms per asymmetric unit) using chemical criteria. Most metal atoms in these types of structures are arranged in Me<sub>6</sub> octahedral clusters which are linked through connected corners or edges. The non-metals are typically found inside trigonal prisms formed by metal atoms (Figs. 1*b* and *c*). The correctness of the structure was proven by refining the atomic coordinates and temperature factors of the nine unique atoms (Table 1) using *SHELXL-97* (Sheldrick, 1998). The final crystallographic  $R$  value was 23.9% for the 28 parameters refined against 170 unique reflections from the single  $h0l$  SAED pattern (Fig. 1*a*). Since the average thickness of the investigated crystal was unknown, no intensity correction for the curvature of the Ewald sphere was applied. Thus, the obtained atomic displacement factors from least-squares

**Table 1**

Refined atomic coordinates and atomic displacement factors of  $\beta$ -Ti<sub>2</sub>Se.

Standard uncertainties are given in parentheses.

	$x$	$y$	$z$	$U_{eq}$ (Å <sup>2</sup> )
Ti1	0.2311 (9)	3/4	0.7565 (20)	0.028 (6)
Ti2	0.3367 (11)	3/4	0.0473 (25)	0.044 (7)
Ti3	0.1463 (10)	3/4	0.0825 (21)	0.031 (6)
Ti4	0.3907 (9)	3/4	0.3516 (19)	0.026 (6)
Ti5	0.0325 (8)	3/4	0.3868 (16)	0.014 (5)
Ti6	0.5145 (13)	1/4	0.3844 (27)	0.055 (8)
Se1	0.2410 (9)	1/4	0.9641 (19)	0.041 (6)
Se2	0.4239 (11)	1/4	0.1600 (21)	0.051 (7)
Se3	0.1260 (10)	1/4	0.2796 (23)	0.050 (6)

refinement covers both the intensity decay due to the excitation error and the true thermal displacement.

The condensed cluster compounds in the Ti–Se system share as common feature a mirror plane that is perpendicular to the short  $b$  axis. Accordingly, the assignment of the atom positions along the short  $b$  axis ( $y = 1/4$  or  $3/4$ ) (Table 1) could be performed using the known topology of condensed octahedral Ti<sub>6</sub> clusters and their combination with capped trigonal prisms of titanium around the selenium. The empirical formula derived from this structure model has 67.7 at.% Ti, close to the 68 (1) at.% found by EDXS. The structure of  $\beta$ -Ti<sub>2</sub>Se is isostructural with the recently described compound Hf<sub>6-x</sub>Mo<sub>x</sub>P<sub>3</sub> (Cheng & Franzen, 1996) and also shares some features with Nb<sub>2</sub>Se (Conard *et al.*, 1969). Comparison of the refined atomic coordinates for  $\beta$ -Ti<sub>2</sub>Se with those published for Hf<sub>6-x</sub>Mo<sub>x</sub>P<sub>3</sub> agreed on average within 0.12 Å.

In order to check if this was just an especially fortunate case or if indeed automated direct methods can be generally applied to experimental electron diffraction data for solving inorganic structures containing heavy elements, we then tried to solve five other metal-rich compounds of varying complexity by applying direct methods to electron diffraction data (Table 2). The metals ranged from titanium ( $Z = 22$ ) to zirconium ( $Z = 40$ ), while the non-metals were lighter; sulfur ( $Z = 16$ ) and selenium ( $Z = 34$ ).

Structures of these five compounds were studied in a similar way to that of  $\beta$ -Ti<sub>2</sub>Se. All these compounds have one short unit-cell axis of about 3.5 Å. SAED patterns were obtained along that prominent axis from these compounds. Electron diffraction patterns were recorded on standard photographic EM films or by a slow-scan CCD camera. For those that were recorded on EM films, an 8-bit video-rate CCD camera (DAGE-MTI model CCD72E) was used for digitizing the photographic negatives. The film data were corrected for the nonlinearity in the blackening curve using a grey step wedge transparent (Eastman Kodak) as reference. Quantification of electron diffraction intensities and structure determination by direct methods were carried out in a similar way to that for  $\beta$ -Ti<sub>2</sub>Se.

For each of the five structures, the potential map with the highest figure of merit showed the correct structure solution with all atoms in projection. In most cases, the highest peaks corresponded to the heavier atoms, *i.e.* the metal atoms, while

the non-metals had lower peaks. However, the final interpretation of the maps was performed mainly on chemical criteria, as described above.

The structures ranged from the rather simple  $\text{Ti}_9\text{Se}_2$  and  $\text{Zr}_2\text{Se}$  with only 6 and 9 unique atoms in the unit cell, respectively, to the more complicated  $\text{Ti}_8\text{Se}_3$  and  $\text{Ti}_{11}\text{Se}_4$  with 22 and 23 unique atoms (Table 2). For each structure, there were between 10 and 40 symmetry-independent reflections per atom, depending on the resolution.

The quality of the data sets used was quite variable (Figs. 1*a*, 2*a* and 3*a*). Although it is difficult to give a quantitative measure of the relative amount of multiply scattered electrons in an electron diffraction pattern, a qualitative estimate is possible. For SAED patterns taken from very thin crystals, the systematically forbidden reflections are hardly visible in the SAED patterns (Fig. 2*a*). Intensities of diffraction spots vary within a great range. Electron diffraction intensities extracted

from such SAED patterns are close to kinematical. In these cases, the atomic positions obtained by direct methods are very accurate before the refinement, compared to those obtained by X-ray single-crystal diffraction (Table 2). An example of a structure determination from high-quality electron diffraction data is demonstrated by  $\text{Zr}_2\text{Se}$  (Fig. 2).

The thicker the crystal is, the more pronounced are the dynamical effects. This results in the weak reflections becoming stronger and the strong reflections relatively weaker and systematically forbidden reflections appearing, for example the odd reflections along screw axes. In very thick crystals, the intensities of all reflections in the same resolution range tend to be practically the same. At that stage, all structural information has been lost, since the information about relative positions of atoms within the unit cell resides in the relative intensities of the diffraction spots. In the case of  $\text{Ti}_9\text{Se}_2$ , the diffraction pattern (Fig. 3*a*) was

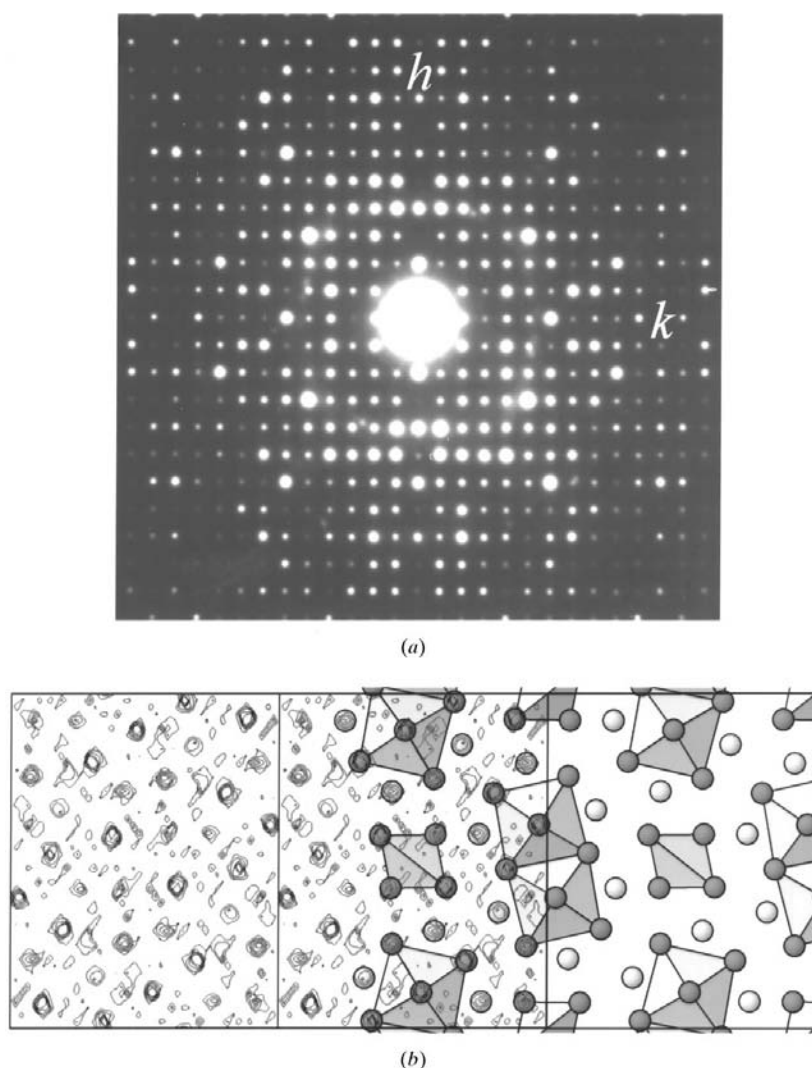


**Figure 2**

(*a*) A SAED pattern of  $\text{Zr}_2\text{Se}$  taken along the short  $c$  axis (projected symmetry  $p2gg$ ). This is an example of a high-quality SAED pattern, as judged by the great range of diffraction intensities and the almost non-existent intensities in the systematically forbidden odd axial reflections. (*b*) The projected potential map of  $\text{Zr}_2\text{Se}$  determined from the SAED data in (*a*). The stronger peaks in the map were assigned to Zr atoms and the weaker peaks to Se atoms. The structure model of  $\text{Zr}_2\text{Se}$  from X-ray crystallography is superimposed on the right part of the potential map. Zr atoms (filled circles) form octahedral clusters while Se atoms (open circles) are located inside trigonal prisms.

clearly severely affected by multiple scattering, as can be seen by comparison with the kinematical diffraction pattern (Fig. 3*b*) calculated from the structure obtained by X-ray crystallography (Weirich, Simon & Pöttgen (1996) using the program *DIFFPAT* (Skarnoulis *et al.*, 1979). Yet there is some resemblance between the experimental and the calculated diffraction patterns, especially the strong reflections, which are strong in both patterns. Since the strong reflections are the most important ones for solving a crystal structure by direct methods, this resemblance may explain why the structure could be solved even from this electron diffraction pattern which results from pronounced dynamical scattering. The accuracy of the atomic positions determined for  $\text{Ti}_9\text{Se}_2$  is

0.2 Å for the Ti atoms and 0.5 Å for the Se atom, much lower than that obtained from a more kinematical electron diffraction pattern (Fig. 2 and Table 2). Needless to say, one should always try to obtain electron diffraction data from the thinnest part of a crystal in order to obtain data as close to kinematical as possible. This example shows that direct methods can be quite robust and tolerate data with a substantial contribution from dynamical scattering. It should be noted, however, that the approximation  $|F_{hkl}| \propto I_{hkl}$  was used in all cases for phenomenological compensation of the dynamical contributions. The common approach  $|F_{hkl}| \propto (I_{hkl})^{1/2}$  yielded in all cases incomplete or wrong structural solutions.

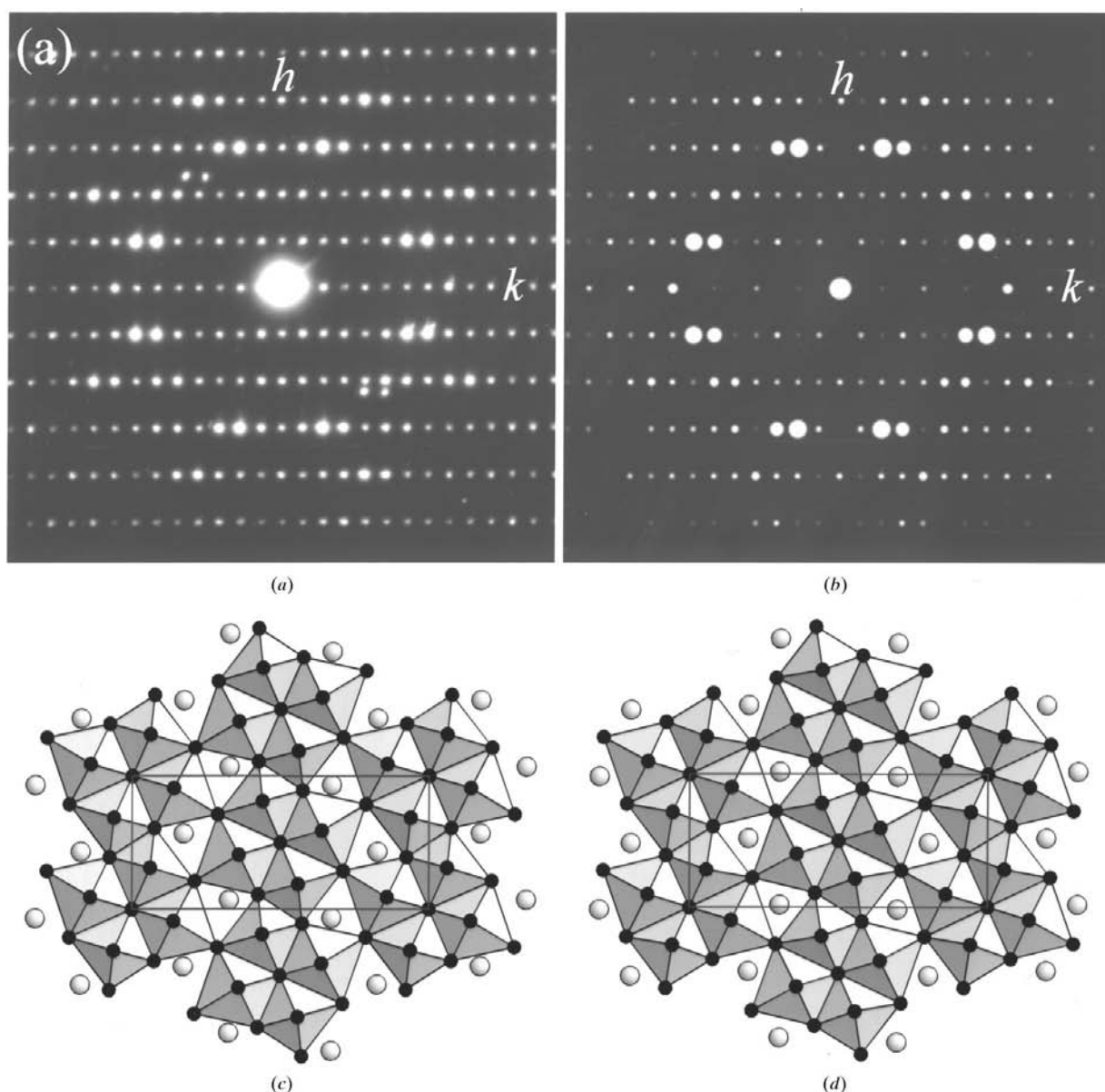


**Figure 3**

(*a*) An experimental selected-area electron diffraction pattern of  $\text{Ti}_9\text{Se}_2$  recorded along the short *c* axis. The experimental pattern is from a rather thick crystal, judged by the fact that the intensities are almost the same for very many reflections including even the forbidden axial reflections. (*b*) The electron diffraction pattern of  $\text{Ti}_9\text{Se}_2$  calculated from the X-ray structure assuming ideal kinematical scattering of electrons. Structure models of  $\text{Ti}_9\text{Se}_2$  obtained by (*c*) electron and (*d*) X-ray crystallography. In spite of the rather poor quality of the SAED pattern, all five unique Ti atoms (filled circles) were correctly found within 0.2 Å. The Se atom (open circles) was off by as much as 0.5 Å, a misplacement that is seen by comparing (*c*) and (*d*).

**Table 2**

Experimental data for the structures solved by direct methods from electron diffraction data (lattice parameters  $a$ ,  $b$ ,  $c$  in Å).

The unit-cell dimensions were obtained from X-ray diffraction, except for the  $a$  and  $c$  axes of  $\beta$ -Ti<sub>2</sub>Se, which were determined from electron diffraction.

Compound	Unit-cell parameters (Å, °)	Space group	Atoms per asymmetric unit	Data from	Number of independent reflections	Crystallographic resolution of the electron data (Å)	Deviation between atomic coordinates obtained by X-rays and electrons†	
							Maximum (Å)	Average (Å)
$\beta$ -Ti <sub>2</sub> Se	$a = 17.934$ (20) $b = 3.453$ (1) $c = 9.526$ (10)	<i>Pnma</i>	9	CCD	170	0.77	‡	‡
Ti <sub>11</sub> Se <sub>4</sub>	$a = 25.516$ (11) $b = 3.4481$ (14) $c = 19.201$ (6) $\beta = 117.84$ (3)	<i>C2/m</i>	23	Film	411	0.75	0.207‡§	0.102‡§
Ti <sub>8</sub> Se <sub>3</sub>	$a = 25.562$ (4) $b = 3.4411$ (5) $c = 19.701$ (6) $\beta = 122.25$ (1)	<i>C2/m</i>	22	CCD	418	0.9	0.161	0.087
Ti <sub>9</sub> Se <sub>2</sub>	$a = 6.917$ (2) $b = 15.505$ (9) $c = 3.454$ (2)	<i>Pbam</i>	6	Film	132	0.8	0.514	0.150
Zr <sub>2</sub> Se	$a = 12.6400$ (27) $b = 15.7968$ (32) $c = 3.6016$ (10)	<i>Pnnm</i>	9	Film	392	0.5	0.103	0.071
Ti <sub>2</sub> S	$a = 11.3507$ (4) $b = 14.0523$ (5) $c = 3.3222$ (1)	<i>Pnnm</i>	9	Film	97	1.0	0.287	0.162

References: Ti<sub>11</sub>Se<sub>4</sub> (Weirich, Ramlau *et al.*, 1996); Ti<sub>8</sub>Se<sub>3</sub> (Weirich, Pöttgen & Simon, 1996); Ti<sub>9</sub>Se<sub>2</sub> (Weirich, Simon & Pöttgen, 1996); Zr<sub>2</sub>Se (Franzen & Norrby, 1968); Ti<sub>2</sub>S (Owens *et al.*, 1967; Weirich, 1996). † The coordinates from X-rays are after least-squares refinement, while those from electrons are directly from the output of SIR97. ‡ No data from X-ray crystallography available. § Coordinates refined with electron diffraction data are compared with those obtained directly from SIR97.

#### 4. Discussion

When the difference in atomic number is very large, it may be difficult to find the lighter atoms. This was the case with Ta<sub>2</sub>P (Weirich *et al.*, 1998) where we found only the heavy Ta atoms ( $Z = 73$ ) by direct methods and could refine them to within 0.01 Å compared to the coordinates obtained by X-ray single-crystal diffraction, but the light P atoms ( $Z = 15$ ) could not be located. Similarly, we have not yet been able to find oxygen atoms in metal oxides, such as niobium oxides. There may be several explanations why the very light atoms are so hard to find with electron diffraction data. Apart from their weaker contribution to the scattering, they may be negatively charged and thus have a negative electron scattering contribution in the low-resolution range (Vainshtein, 1964). The electron scattering-factor tables may need to be improved, especially for charged atoms. Correction for multiply scattered electrons (Jansen *et al.*, 1998) was not performed here, but may be necessary especially for more demanding cases and precise structure refinement. On the other hand, the good agreement between the coordinates obtained for  $\beta$ -Ti<sub>2</sub>Se from electron diffraction and the result for Hf<sub>6-x</sub>Mo<sub>x</sub>P<sub>3</sub> from single-crystal X-ray data indicates that the atomic positions from SAED are already very close to the 'true' coordinates. Introducing dynamical corrections is expected to yield only minor changes.

The fact that crystal structures can be solved directly from real experimental electron diffraction patterns overthrows the dogma of electron diffraction data from crystals composed of strongly scattering heavy atoms being useless (Cowley, 1993; Williams & Carter, 1996). It does not, of course, show that

dynamical scattering does not occur. It only shows that in spite of dynamical scattering the electron diffraction data can be sufficiently good (*i.e.* sufficiently close to kinematical) to allow the structure to be solved, if only reasonable care has been taken to collect the diffraction data from a rather thin crystal, so that the characteristic intensity alterations in the diffraction pattern are preserved. It is also worth emphasizing that compensation for dynamical diffraction can only be applied if a structure model already exists, as part of calculations of images and diffraction patterns, using for example the multi-slice approach. Thus, there is no way to correct the raw data for the multiply scattered electrons by model calculations before the structure has been solved. The present study opens the possibility of applying any elaborate correction for dynamical effects to many new crystal structures.

#### 5. Conclusions

The possibility of quasi-automatic solving of unknown structures by direct methods from electron diffraction data, collected with standard instruments, moves electron crystallography from a specialized technique for experts towards a routine method. This overcomes the limitation of X-ray diffraction studies on extremely small (nanosized) crystals and widens the possibilities for structure investigations to the vast number of materials that can only be synthesized as sub-micrometre crystalline powders, such as catalysts, precipitates in alloys and many technically important nanocrystalline materials.

We are grateful to Miss Viola Duppel (MPI, Stuttgart) for EDXS analysis and collecting electron diffraction patterns on the slow-scan CCD camera. TEW thanks the Wenner–Gren Foundation for Scientific Research, Stockholm, for financial support. This project was supported by the Swedish Natural Science Research Council (NFR).

## References

- Altomare, A., Burla, M. C., Camalli, M., Cascarano, G., Giacovazzo, C., Guagliardi, A., Moliterni, A. G. G., Polidori, G. & Spagna, R. (1999). *J. Appl. Cryst.* **32**, 115–118.
- Cheng, J. & Franzen, H. F. (1996). *J. Solid State Chem.* **121**, 362–371.
- Conard, B. R., Norrby, L. J. & Franzen, H. F. (1969). *Acta Cryst.* **B25**, 1729–1736.
- Cowley, J. M. (1992). *Electron Diffraction Techniques*, Vol. 1, edited by J. M. Cowley, pp. 1–74. Oxford University Press.
- Cowley, J. M. (1993). *International Tables for Crystallography*, Vol. B, edited by U. Shmueli, p. 280. Dordrecht: Kluwer Academic Publishers.
- DeRosier, D. J. & Klug, A. (1968). *Nature (London)*, **217**, 130–134.
- Dorset, D. L. (1995). *Structural Electron Crystallography*. New York: Plenum Press.
- Dorset, D. L. (1996). *Acta Cryst.* **B52**, 753–769.
- Dorset, D. L. (1998). *Acta Cryst.* **A54**, 750–757.
- Franzen, H. F. & Norrby, L. J. (1968). *Acta Cryst.* **B24**, 601–603.
- Giacovazzo, C. (1998). *Direct Phasing in Crystallography. Fundamentals and Applications*. Oxford University Press.
- Gjønnnes, J., Hansen, V., Berg, B. S., Runde, P., Cheng, Y. F., Gjønnnes, K., Dorset D. L. & Gilmore, C. J. (1998). *Acta Cryst.* **A54**, 306–319.
- Jansen, J., Tang, D., Zandbergen, H. W. & Schenk, H. (1998). *Acta Cryst.* **A54**, 91–101.
- Jiang, J. S. & Li, F. H. (1984). *Acta Phys. Sin.* **33**, 845–849.
- Nicolopoulos, S., Gonzales-Calbet, J. M., Vallet-Regi, M., Corma, A., Corell, C., Guil, J. M. & Perez-Pariente, J. (1995). *J. Am. Chem. Soc.* **117**, 8947–8956.
- Owens, J. P., Conard, B. R. & Franzen, H. F. (1967). *Acta Cryst.* **23**, 77–82.
- Sheldrick, G. M. (1998). *SHELXL-97-2. Program for Crystal Structure Refinement*. University of Göttingen, Germany.
- Simon, A. (1997). *Angew. Chem. Int. Ed. Engl.* **36**, 1788–1806.
- Sinkler, W., Bengu, E. & Marks, L. D. (1998). *Acta Cryst.* **A54**, 591–605.
- Skarnoulis, A. J., Liljestrand, L. & Kihlberg, L. (1979). *Chem. Commun.* **1**, 1–27.
- Vainshtein, B. K. (1964). *Structure Analysis by Electron Diffraction*. Oxford: Pergamon Press.
- Vainshtein, B. K., Zvyagin, B. B. & Avilov, A. S. (1992). *Electron Diffraction Techniques*, Vol. 2, edited by J. M. Cowley, pp. 216–312. Oxford University Press.
- Weirich, T. E. (1996). PhD Thesis, Universität Osnabrück, Germany.
- Weirich, T. E., Hovmöller, S., Kalpen, H., Ramlau, R. & Simon, A. (1998). *Crystallogr. Rep.* **43**, 956–967.
- Weirich, T. E., Pöttgen, R. & Simon, A. (1996). *Z. Kristallogr.* **212**, 929–930.
- Weirich, T. E., Ramlau, R., Simon, A., Hovmöller, S. & Zou, X. D. (1996). *Nature (London)*, **382**, 144–146.
- Weirich, T. E., Simon, A. & Pöttgen, R. (1996). *Z. Anorg. Allg. Chem.* **622**, 630–634.
- Williams, D. B. & Carter, C. B. (1996). *Transmission Electron Microscopy*, Vol. 2, p. 203. New York: Plenum Press.
- Zou, X. D., Sukharev, Y. & Hovmöller, S. (1993). *Ultramicroscopy*, **52**, 436–444.